

# Mössbauer study of vacuum annealed $\text{Fe}_{100-x}\text{Ga}_x$ ( $10 \leq x \leq 35$ ) thin films

Tadeusz Szumiata,  
Bogumił Górka,  
Katarzyna Brzózka,  
Michał Gawroński,  
Małgorzata Gzik-Szumiata,  
Athar Javed,  
Nicola A. Morley,  
Mike R. J. Gibbs

**Abstract.** This work reports results from comparative Mössbauer studies of as-deposited and annealed  $\text{Fe}_{100-x}\text{Ga}_x$  ( $10 \leq x \leq 35$ ) high magnetostrictive thin films of constant thickness ( $50 \pm 2$  nm). Films were grown on Si(100) substrates using a co-sputtering and evaporation chamber where Fe has been sputtered and Ga was evaporated. During growth of films, a magnetic field of 65 kA/m has been applied in the plane of the film. Annealed films have been obtained by heating in vacuum for 1 h at 350°C without magnetic field. After annealing, the saturation field of the Fe-Ga films has been significantly reduced. By means of the  $^{57}\text{Fe}$  CEMS technique the contributions from several phases have been found: Fe-Ga A2 (bcc), traces of  $\text{DO}_3$  phase, a gallium-rich disordered phase and iron oxides (both goethite and magnetite). For the sample with  $x = 26.5$  the heat treatment reduces the  $\text{DO}_3$  phase content whereas for the film with  $x = 16.4$  the opposite tendency has been observed. Mössbauer results were compared with XRD and MOKE findings.

**Key words:** Fe-Ga • thin films • CEMS • MOKE

T. Szumiata✉, B. Górka, K. Brzózka, M. Gawroński,  
M. Gzik-Szumiata  
Technical University of Radom,  
Department of Physics,  
54 Krasickiego Str., 26-600 Radom, Poland,  
Tel.: +48 48 361 7846, Fax: +48 48 361 7075,  
E-mail: t.szumiata@pr.radom.pl,  
t.szumiata@hotmail.com

A. Javed  
University of the Punjab,  
Department of Physics,  
Quaid-i-Azam Campus, Lahore-54590-Pakistan

N. A. Morley, M. R. J. Gibbs  
University of Sheffield,  
Department of Materials Science & Engineering,  
Sheffield S1 3JD, UK

Received: 11 June 2012  
Accepted: 18 October 2012

## Introduction

Fe-Ga thin films [6, 7, 10, 11] are famous for their high magnetostriction, low saturation field, low coercivity, and have applications in magnetic microelectromechanical systems (MagMEMS) [3]. Their properties make them promising candidates for use in strain sensor devices [4]. Studies on bulk Fe-Ga alloys point to high sensitivity of their magnetostriction to  $\text{DO}_3$ -type ordering [12]. The presence of this phase can be effectively monitored by means of Mössbauer spectrometry [2]. Previous studies of Fe-Ga thin films [6, 7, 10] showed no traces of the ordered  $\text{DO}_3$  or  $\text{L}_{12}$  phases. The main goal of present work is to investigate the influence of annealing process on structural, magnetic and magnetoelastic properties of  $\text{Fe}_{100-x}\text{Ga}_x$  thin films fabricated in the presence of magnetic field ( $\approx 65$  kA/m). Strong motivation for annealing of Fe-Ga films is an expected decrease in their saturation field  $H_s$ .

## Experimental

$\text{Fe}_{100-x}\text{Ga}_x$  ( $10 \leq x \leq 35$ ) films were grown on Si(100) substrates using a specially designed co-sputtering and evaporation chamber where Fe was sputtered and Ga was evaporated [9]. Before deposition, the Si(100) substrates were ultrasonically cleaned with acetone and isopropanol to ensure that the substrate is free from contamination. During deposition, a pressure of the Ar working gas was set to  $p_{\text{Ar}} = 4$   $\mu\text{bar}$  and Ga evaporation rate was fixed ( $R_{\text{Ga}} = 0.3$  – see [9]) while Fe sputter power  $P_{\text{Fe}}$  was varied to achieve Fe-Ga films with different Fe to Ga ratio. During

the growth process, a forming field of  $\sim 65 \text{ kA}\cdot\text{m}^{-1}$  was applied in the plane of the film in order to introduce directional order and an induced magnetic anisotropy. After deposition, the samples were annealed in vacuum ( $1.4 \times 10^{-5} \text{ mbar}$ ). The films were heat treated for 1 h at  $350^\circ\text{C}$ . After annealing, the films were allowed to cool down to room temperature under vacuum with no field applied. It should be noted that the annealing temperature was chosen on the basis of Wang *et al.* work [11]. Their study showed that an annealing temperature greater than  $350^\circ\text{C}$  caused a significant decrease in magnetostriction of  $\text{Fe}_{81}\text{Ga}_{19}$  films. Our films were  $(50 \pm 2) \text{ nm}$  thick. The films thickness was measured by a crystal monitor placed near the substrate. The achieved thickness was later confirmed in the analysis of cross-sectional scanning electron microscope (SEM) images as well as using an atomic force microscope (AFM).

Microstructure of the films was studied using a standard X-ray diffraction (XRD) technique. X-ray diffractometer (Siemens) with Co radiation (wavelength,  $\lambda = 1.7896 \text{ \AA}$ ) was used in  $\theta$ - $2\theta$  mode to collect XRD spectra of all films. The composition of all films was studied using energy dispersive X-ray spectroscopy (EDS). Magnetic properties were studied using a transverse magneto-optic Kerr effect (MOKE) magnetometer. The effective saturation magnetostriction constant ( $\lambda_{\text{eff}}$ ) was measured using the Villari effect. This involved straining each film over bending tools of different known radii,  $R$ . The detail of the procedure of measuring  $\lambda_{\text{eff}}$  is described elsewhere [7]. Room temperature  $^{57}\text{Fe}$  conversion electron Mössbauer spectrometry (CEMS) was applied in order to identify the phases. In the CEMS experiments the  $^{57}\text{Co}:\text{Rh}$  source was fixed to the vibrator operating in a constant acceleration mode. The resonant electrons generated by the internal conversion process after the absorption of Mössbauer  $\gamma$ -rays were counted with a gas flow type conversion electron detector. CEMS spectra were fitted with Voigt-type functions (Zeeman sextets with Lorentzian lines convoluted with Gaussian hyperfine field distributions) by means of dedicated PolMöss software [7, 10] based on MS Excel Solver gradient-genetic optimization procedures.

## Results and discussion

XRD measurements demonstrate that all annealed  $\text{Fe}_{100-x}\text{Ga}_x$  films had strong  $\langle 110 \rangle$  texture normal to the film plane similar to the as-deposited films. For both film sets (annealed and as-deposited  $\text{Fe}_{100-x}\text{Ga}_x$  films), the lattice constant was determined from the  $\langle 110 \rangle$  peak position. For as-deposited  $\text{Fe}_{100-x}\text{Ga}_x$  films, it was found that the lattice constant rose with an increase in Ga composition (Fig. 1) which is consistent with our earlier studies [5–7]. However, for the annealed films, the lattice constant increased with Ga composition up to 22 at.% Ga (Fig. 1). For  $x > 22$ , the lattice shrank with Ga content. This is most likely due to a small amount of Ga be evaporated on annealing causing a decrease in lattice parameter (see later).

Figure 2 shows the saturation field,  $H_s$ , as a function of Ga composition for annealed and as-deposited

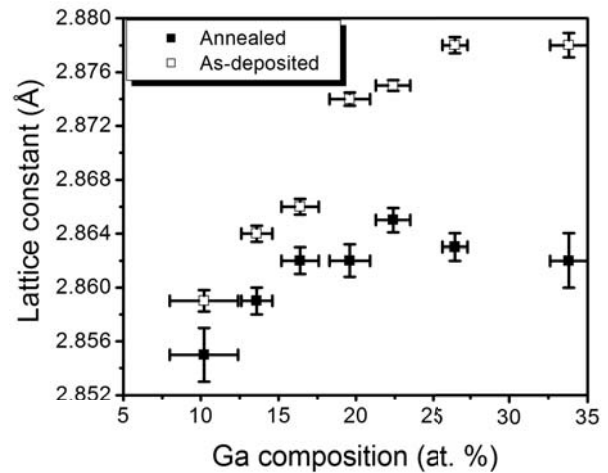


**Fig. 1.** Lattice constant as a function of Ga composition for  $\text{Fe}_{100-x}\text{Ga}_x$  films (■) annealed at  $350^\circ\text{C}$  for 1 h (□) as-deposited.

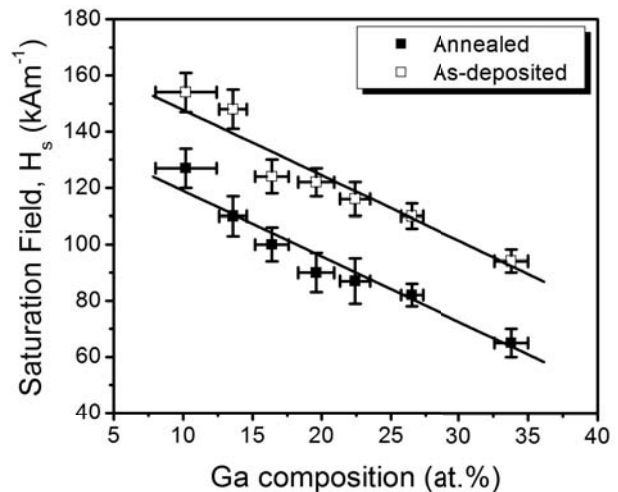


**Fig. 2.** Saturation field as a function of Ga composition for  $\text{Fe}_{100-x}\text{Ga}_x$  films (■) annealed at  $350^\circ\text{C}$  for 1 h (□) as-deposited. The straight line on each data set is a guide for the eye.

$\text{Fe}_{100-x}\text{Ga}_x$  films. After annealing, it was found that the saturation field,  $H_s$ , over the whole range of composition was significantly reduced ( $\sim 40 \text{ kA}\cdot\text{m}^{-1}$ ) comparing with the as-deposited Fe-Ga films. Figure 3 presents the effective saturation magnetostriction,  $\lambda_{\text{eff}}$  as a function of Ga composition for annealed and as-deposited  $\text{Fe}_{100-x}\text{Ga}_x$  films. For  $x < 20$ , the saturation magnetostriction,  $\lambda_{\text{eff}}$  was found to be similar (within an experimental error) in both annealed and as-deposited films. For  $x > 20$ , it was found that the annealed  $\text{Fe}_{100-x}\text{Ga}_x$  films has lower magnetostriction as compared with the as-deposited films. A decrease in  $\lambda_{\text{eff}}$  may be due to an increase in grain size and precipitation of  $\text{DO}_3$  phase (not detected by XRD, but visible in CEMS spectra – see later) that occurs during annealing. This is consistent with the results of Wang *et al.* [11], where they also studied the effect of annealing temperature ( $300^\circ\text{C}$  to  $500^\circ\text{C}$ ) on the magnetostriction in  $\text{Fe}_{81}\text{Ga}_{19}$  films. Further, it can be seen that the  $\lambda_{\text{eff}}$  data of annealed films (for  $x < 20$ ) is in good agreement with the  $\lambda_{\langle 110 \rangle}$  textured curve (see Fig. 3) while for  $x > 20$ , the  $\lambda_{\text{eff}}$  is significantly lower compared with the  $\lambda_{\langle 110 \rangle}$  in  $\text{Fe}_{100-x}\text{Ga}_x$  alloys having strong  $\langle 110 \rangle$  texture.

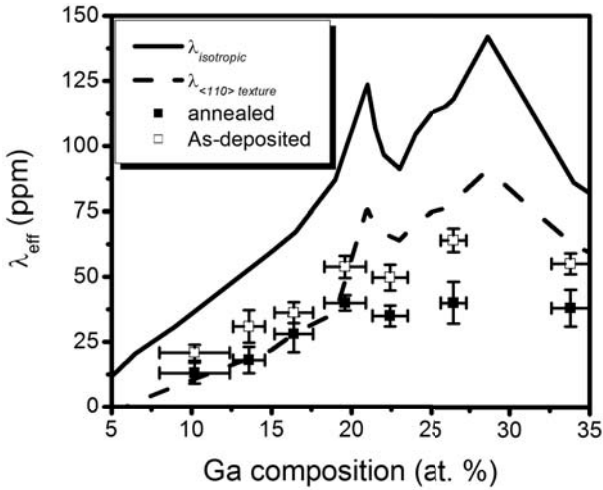


**Fig. 3.** The effective saturation magnetostriction ( $\lambda_{\text{eff}}$ ) as a function of Ga composition for  $\text{Fe}_{100-x}\text{Ga}_x$  films (■) annealed at  $350^\circ\text{C}$  for 1 h (□) as-deposited. The as-deposited (□)  $\lambda_{\text{eff}}$  data were taken from Ref. [1] to compare it with annealed thin film data. The solid and dashed curve represents the calculated magnetostriction for isotropic and  $\langle 110 \rangle$  textured  $\text{Fe}_{100-x}\text{Ga}_x$  alloy respectively.

Room temperature  $^{57}\text{Fe}$  CEMS spectra (Fig. 4) for the samples of two different Ga contents ( $x = 16.4$  and  $x = 26.5$ ) were fitted with several distributions of the hyperfine magnetic field (Fig. 5). Main two components (G01 and G02) correspond to Fe-Ga A2 (bcc) phase. The first one (hyperfine field  $B_{\text{hf}} \approx 33$  T) describes the contribution of Fe atoms in Fe-Ga disordered alloy which possess 8 Fe atoms as nearest neighbours. The second one is characterized by  $B_{\text{hf}}$  value about 3 T lower than that for G01 (and twice higher standard deviation). Its hyperfine field is significantly higher than 27 T ex-

pected for the fcc  $L1_2$  phase [8]. Thus G02 component comes from these Fe atoms for which a replacement of one or two Fe atoms by Ga ones occurred in the first neighbour shell in A2 structure [1]. G03 and G04 subspectra correspond to the  $\text{DO}_3$  phase [2]. For all previously studied Fe-Ga thin films [6, 7, 10] by means of CEMS no contribution of  $\text{DO}_3$  phase was found. A possible reason for this difference could be the fact that the present samples were fabricated by applying a forming field during growth, which could impose an additional ordering. For the sample with  $x = 26.5$ , the heat treatment reduces  $\text{DO}_3$  phase content from about 7% to 4%, whereas in case of the film with  $x = 16.4$  the opposite tendency was observed (increase from 4% to 11%). A low field component G05 could be assigned to gallium-rich disordered regions. Heat treatment promotes a creation of this phase in the sample of lower Ga content – contrary to the case of the sample of higher Ga content. In all samples traces of iron oxide (goethite) were discovered (component G06, 3–8%). In case of annealed films a significant contribution (16–25%) of magnetite was observed (components G07 and G08) which points to the imperfect vacuum during annealing. The investigated samples had no capping layer; which is why they were susceptible to oxidation.

An important consequence of the annealing is an apparent drop of G02 (lower field component of A2 phase) relative to G01 component. It suggests a possible evaporation or precipitation of some amount of gallium. This effect is very pronounced for the sample with high gallium content ( $x = 26.5\%$ ) in which a G01/G02 contributions ratio changes more than 9 times. In all samples the line amplitudes ratio in distributed Zeeman sextets points to the almost in-plane spin configuration (no more than  $20^\circ$  deviation) – especially in case of the

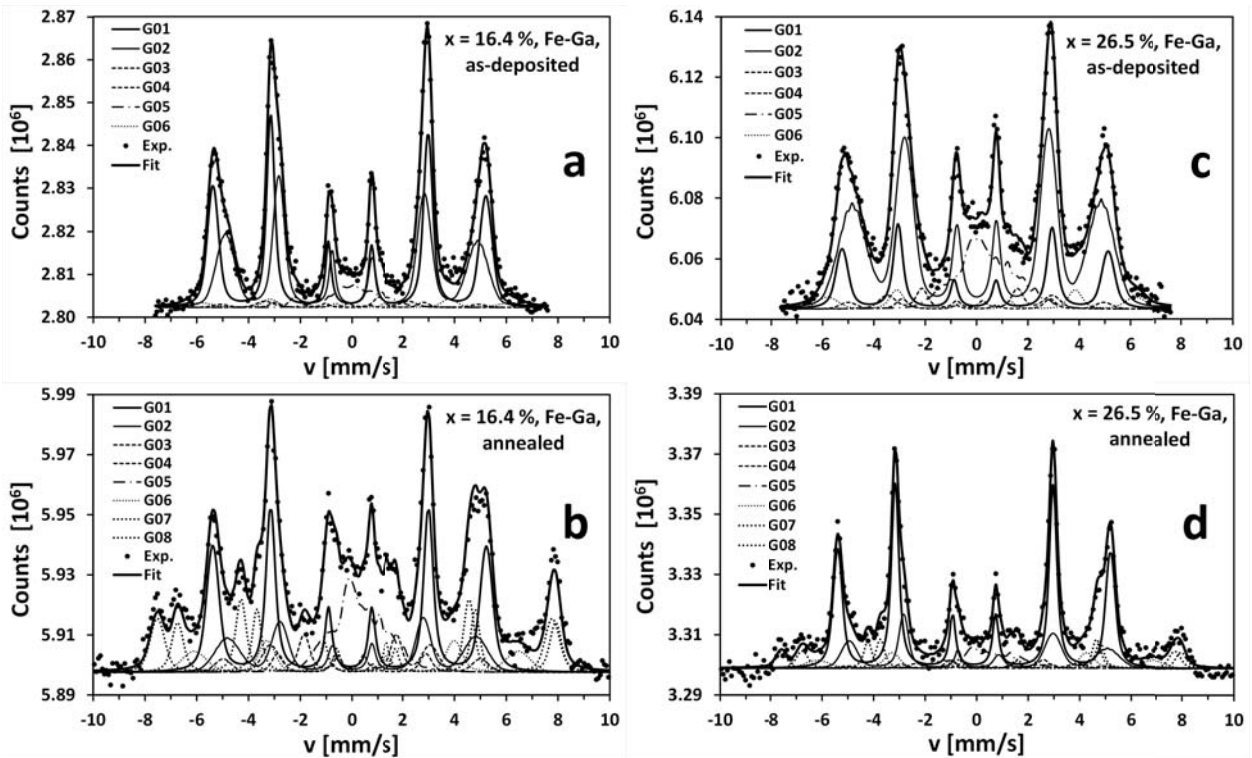


**Fig. 4.** CEMS spectra for  $\text{Fe}_{100-x}\text{Ga}_x$  films: (a)  $x = 16.4\%$ , as-deposited; (b)  $x = 16.4\%$ , annealed; (c)  $x = 26.5\%$ , as-deposited; (d)  $x = 26.5\%$ , annealed.

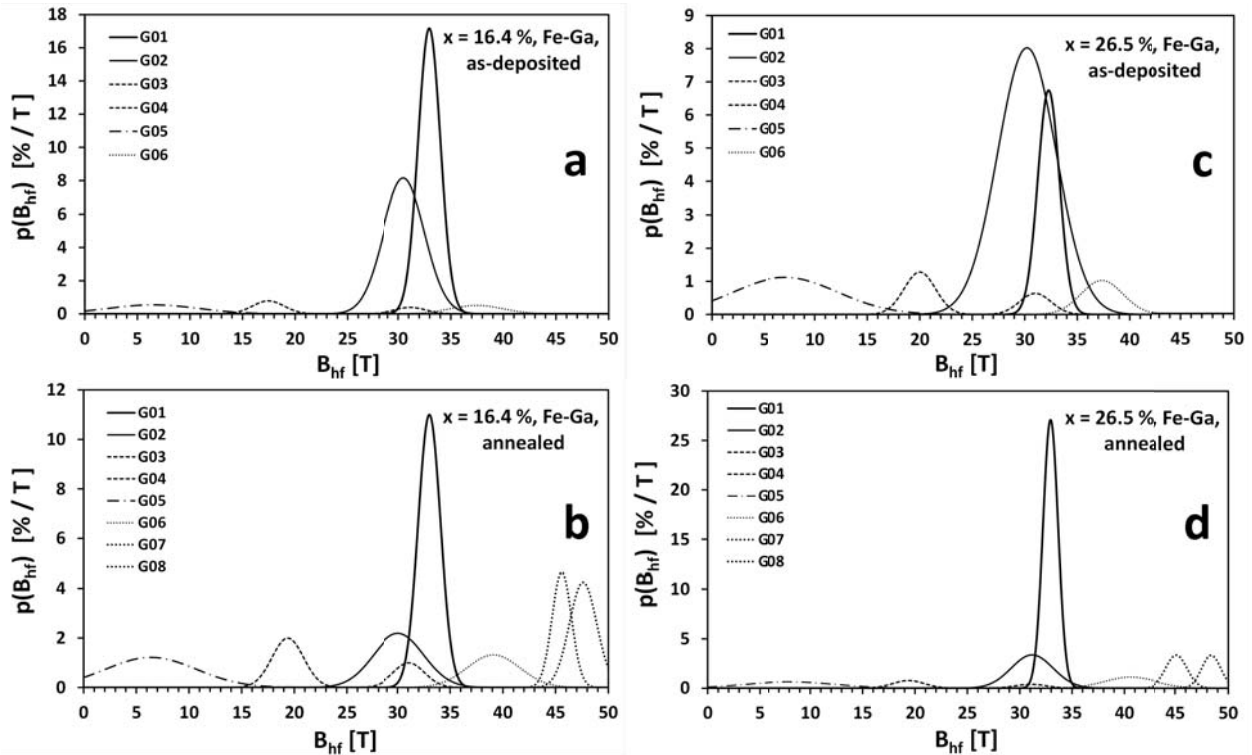


**Fig. 5.** Hyperfine field distributions for  $\text{Fe}_{100-x}\text{Ga}_x$  films: (a)  $x = 16.4\%$ , as-deposited; (b)  $x = 16.4\%$ , annealed; (c)  $x = 26.5\%$ , as-deposited; (d)  $x = 26.5\%$ , annealed.

annealed film with  $x = 26.5\%$  (just  $3^\circ$  deviation). Isomer shift (IS) values for two main components G01 and G02 were linearly correlated with Gaussian distributions of the hyperfine magnetic field. The quadrupole splitting QS was fixed to zero for the components G01-G04 which corresponds to the phases of cubic symmetry structure.

## Conclusions

Annealing process of Fe-Ga films causes noticeable changes of their structural and magnetic properties, which were effectively studied by CEMS, XRD and MOKE techniques. As expected, a saturation field was reduced, however effective saturation magnetostriction dropped presumably due to partial evaporation of the gallium during heating (which was confirmed by CEMS). No change in crystalline texture was observed.  $\text{DO}_3$  phase amount evolution was dependent on gallium content. For gallium rich Fe-Ga films, the heating process as well as forming field during deposition favoured in-plane spin configuration, which is very important for MagMEMS and sensor applications.

## References

1. Błachowski A, Ruebenbauer K, Żukrowski J, Przewoźnik (2008) Charge and spin density on iron nuclei in the BCC Fe-Ga alloys studied by Mössbauer spectroscopy. *J Alloys Compd* 455:47–51
2. Borrego JM, Blázquez JS, Conde CF, Conde A, Roth S (2007) Structural ordering and magnetic properties of arc-melted FeGa alloys. *Intermetallics* 15:193–200
3. Gibbs MRJ (2007) Materials optimization for magnetic MEMS. *IEEE Trans Magn* 43:2666–2671
4. Hattrick-Simpers JR, Hunter D, Craciunescu CM *et al.* (2008) Combinatorial investigation of magnetostriction in Fe-Ga and Fe-Ga-Al. *Appl Phys Lett* 93:102507 (3 pp)
5. Javed A, Morley NA, Gibbs MRJ (2009) Structure, magnetic and magnetostrictive properties of as-deposited Fe-Ga thin films. *J Magn Magn Mater* 321:2877–2882
6. Javed A, Morley NA, Szumiata T, Gibbs MRJ (2011) A comparative study of the microstructural and magnetic properties of  $\langle 110 \rangle$  textured thin polycrystalline  $\text{Fe}_{100-x}\text{Ga}_x$  ( $10 \leq x \leq 35$ ) films. *Appl Surf Sci* 257:5977–5983
7. Javed A, Szumiata T, Morley NA, Gibbs MRJ (2010) An investigation of the effect of structural order on magnetostriction and magnetic behavior of Fe-Ga alloy thin films. *Acta Mater* 58:4003–4011
8. Kawamiya N, Adachi K, Nakamura YJ (1970) Magnetic properties and Mössbauer investigations of Fe-Ga alloys. *Phys Soc Jpn* 33:1318–1327
9. Morley NA, Yeh S-L, Rigby S, Javed A, Gibbs MRJ (2008) Development of a co-sputter-evaporation chamber for Fe-Ga films. *J Vac Sci Technol A* 20:581–586
10. Szumiata T, Brzózka K, Gawroński M *et al.* (2011) Structural and magnetic ordering in Fe-Ga thin films examined by Mössbauer spectrometry. *Acta Phys Pol A* 119:21–23
11. Wang BW, Li S, Zhou Y, Huang WM, Cao SY (2008) Structure, magnetic properties and magnetostriction of  $\text{Fe}_{81}\text{Ga}_{19}$  thin films. *J Magn Magn Mater* 320:769–773
12. Xing Q, Du Y, McQueeney RJ, Lograsso TA (2008) Structural investigations of Fe-Ga alloys: Phase relations and magnetostrictive behavior. *Acta Mater* 56:4536–4546